Transportation Research Part E 61 (2014) 192–211

Contents lists available at ScienceDirect

Transportation Research Part E

journal homepage: www.elsevier.com/locate/tre

The design of coastal shipping services subject to carbon emission reduction targets and state subsidy levels

Kang Chen [a,1], Zhongzhen Yang [a,2], Theo Notteboom [b,*]

[a] Transportation Management College, Dalian Maritime University, 1 Linghai Road, Dalian, Liaoning, China
[b] Institute of Transport and Maritime Management Antwerp (ITMMA), University of Antwerp, Kipdorp 59, 2000 Antwerp, Belgium

ARTICLE INFO

Article history:
Received 4 April 2013
Received in revised form 4 October 2013
Accepted 10 November 2013

Keywords:
Intermodal transport
Liner route design
User equilibrium
Genetic algorithm
Carbon emission
State subsidy

ABSTRACT

This paper presents a New Coastal Liner Route Design Model (NCLRDM) for coastal intermodal networks based on the user equilibrium assignment model (UE model). The NCLRDM can determine ports of call, call sequence, ship type and service frequency simultaneously with the objective of minimizing state subsidies for coastal shipping operators under a given carbon emission reduction target for the entire intermodal network. A network-topology method (Temporal–Spatial Expansion) captures differences in traffic assignment between waterway and highway networks. A genetic and Frank–Wolfe hybrid algorithm is used to solve the NCLRDM. The model is applied to the Bohai Bay in China.

1. Introduction

1.1. Background

Coastal liner shipping is a crucial component of the transport system in coastal regions. It is only since the late 1980s that coastal shipping has been recognized as a genuine sector with specific properties, specific problems and a specific task in regional freight mobility. In Europe, increased European integration, growing intra-European trade and a focus on an environment-friendly modal split led to a renewed interest in coastal shipping both in logistics and transport policy-making. In Asia, growing intra-regional trade and fast economic development have urged policy makers and market players to promote the use of coastal services. In the US, many impediments in American shipping regulations gravitating around the US Merchant Marine Act of 1920 (also known as the Jones Act) have led to only limited services between American ports. The Jones Act, which basically states that cargo may not be transported between two US ports unless it is transported by vessels owned by citizens of the US, built and registered in the US, and manned by a crew of US nationals, implies that the potential of domestic shipping in North America remains underutilized (Brooks and Trifts, 2008). During the last 50 years, the Jones Act has been revised many times, and the most recent version is the re-codified version of 2006. Invariably, the purpose is the same: to support the US coastal shipping industry.

Coastal shipping faces fierce competition from truck services in many regions around the world (García-Menéndez and Feo-Valero, 2009; Ng, 2009; Notteboom, 2011). Still, policy-makers and market players have also come to realize that the

* Corresponding author. Tel.: +32 3 2655149.
E-mail addresses: chenkang@dlmu.edu.cn (K. Chen), yangzhongzhen@dlmu.edu.cn (Z. Yang), theo.notteboom@ua.ac.be (T. Notteboom).
[1] Tel.: +86 411 84723969.
[2] Tel.: +86 411 84726756.

1366-5545/$ - see front matter © 2013 Elsevier Ltd. All rights reserved.
http://dx.doi.org/10.1016/j.tre.2013.11.004

biggest potential for coastal shipping is not found in a direct confrontation with road transport through 'the modal shift' idea, but in its complementary function to road transportation and other modes (López-Navarro et al., 2011). This is where the relevance of the concepts of co-modality and synchro-modality come into play. It has also been recognized that coastal shipping can significantly contribute to a decrease in greenhouse gas emissions in coastal areas (Perakis and Denisis, 2008).

Coastal shipping operators are challenged to develop efficient services using larger ships, raising service frequency and increasing the number of ports of call. However, coastal shipping operators seldom do this voluntarily as such measures typically raise the operating cost. In many cases, the increased cost can hardly be offset by the benefits induced by the increased market scale (García-Menéndez and Feo-Valero, 2009). Facing this situation, some governments have introduced incentive policies. For example, the European Commission developed the Motorways of the Sea program with specific rules on State aid and Community funding (European Union, 2008; Douet and Cappuccilli, 2011). In the US, the "America's Marine Highway Program" is implemented to mitigate landside congestion and to reduce greenhouse gas emissions per ton-mile of freight moved in the Great Lakes/Saint Lawrence Seaway System, intra-coastal and coastal waterways (MARAD, 2011). In both cases, governments underline that the full range of public benefits of coastal services cannot be realized based solely on market-driven transportation choices. Hence, the development of a range of legislation and regulatory actions and financial support programs. These measures are aimed at helping operators to improve services, to introduce new coastal services, to raise the modal share of coastal shipping and to reduce the emissions generated by the entire regional transport system.

Therefore, the design of coastal liner services is not only a task for the operators, but may be influenced by governmental measures in the area of environmental policy and financial incentives. A competitive coastal liner service generates an operating profit and reduces carbon emissions with fewer or no subsidies.

1.2. Scope and aim of the paper

This paper analyzes two critical problems linked to the above discussion on the competitiveness and efficiency of coastal liner services: (a) how to design an efficient coastal liner service given a pre-determined carbon emission reduction goal; (b) how to determine the subsidy needed (if any) in order to minimize the operating loss of coastal service operations on a specific route. We introduce a Coastal Liner Route Design (CLRD) model whereby the objective function is aimed at minimizing the operators' loss and minimizing the need for state subsidies. The resulting complex CLRD problem is deeply affected by the ports of call, the call sequence, the ship type, the service frequency, and the traffic flow on the intermodal transport network (highway and maritime transport). Among them, the traffic flow is most crucial as it determines both the profit of the operators and the carbon emissions in the whole transport system. Thus, we propose to use traffic assignment on the intermodal transport network as the technical basis for the CLRD.

Several theories and application methods exist dealing with the traffic assignment problem. The User Equilibrium (UE) model is widely accepted. However, in order to utilize the UE model, one needs to know the "impedance function" of the links in the network. The function should be monotonous and differentiable. For highway links, the Bureau of Public Roads (BPR) function has been formulated (Sheffi, 1984). However, existing literature does not offer any insights on the impedance function for maritime or waterway links. If the differences between waterway and highway links are not considered, the results of the UE model might deviate significantly from the actual situation.

There are two key differences between highway and waterway links. First of all, a highway link is a facility corridor. Theoretically, it can be used by any user (cargo) at any time. A waterway link is a service channel, which consists of "ship" and "route". As liner ships sail on a fixed route between fixed ports of call on a regular pre-determined basis, the liner sailing schedule will determine the use of the waterway link. For example, if some cargos do not make it to the ship in time, they cannot be transported immediately and have to wait for the next ship. This feature is called "Periodic Connectivity (PC)". Secondly, all users of a highway link have the same or at least a very comparable travel speed. When congestion occurs, the speed of all users on the link will decrease by the same amount. However, congestion on a waterway link implies that the traffic volume is greater than the ship's capacity. When congestion occurs, the loaded cargos are still able to pass the link at normal speed, but for the cargos not loaded, the travel speed is zero. This feature of waterway links is referred to as the Asynchronous Change of Travel Speed (ACTS). PC and ACTS have to be taken into account when assigning traffic flows on an intermodal network.

Considering the two specific features of waterway/maritime links, this paper studies the CLRD from the perspective of state subsidy reduction, and develops a New Coastal Liner Route Design Model (NCLRDM) to optimize the selection of ports of call, the call sequence, the ship type and the service frequency simultaneously, with the objective of minimizing state subsidies.

First, we utilize a network-topology method (i.e. Temporal–Spatial Expansion) to deal with the PC and ACTS problems. This method can improve the reliability of the results of the UE model, and more importantly, it provides a simple, effective and realistic avenue for assigning traffic on liner-like networks, which are formed by large capacity transport units operating on fixed paths on a regular scheduled basis (e.g. railway transport networks or air transport networks). Next, we present the expression of the NCLRDM, and develop a Genetic and Frank–Wolfe Hybrid Algorithm (GFWHA) to solve the model.

The remainder of this paper is organized as follows: Section 2 reviews the relevant literature. Section 3 proposes the method of Temporal–Spatial Expansion and defines the impedance functions of the highway and waterway links. Section 4 develops the NCLRDM. Section 5 presents the GFWHA. Section 6 presents a numerical test to examine the model and the

algorithm with real data collected from the Bohai Bay area in northeast China. Finally, Section 7 contains the conclusions of the study.

2. Literature review

2.1. Traffic assignment subject to PC and ACTS

Transport networks whose links show the PC property are known as "congested transit networks". This type of network was first identified by Last and Keak (1976). Until now, researchers have already presented many traffic assignment methods for the congested transit network, for example: Spiess and Florian (1989), De Cea and Fernández (1993) and Wu et al. (1994). Lam et al. (1999) proposed a stochastic user equilibrium assignment model. By using Lagrange multipliers, their model shows route selection for traffic flows and the travel cost simultaneously. A similar problem was also studied by Cominetti and Correa (2001) and Schmöcker et al. (2008).

The above methods are effective for analyzing high-frequency and low-punctuality transport systems. However, as these methods do not consider service schedules, they are not appropriate for low-frequency and high-punctuality transport systems, where the links have some schedule-sensitive features, such as the ACTS (Nuzzolo et al., 2001). This methodological limitation was overcome by some scholars who introduced the schedule factor into the traffic assigning process, for example: Wong and Tong (1998), Tong and Wong (2000), Nuzzolo and Russo (1996), Florian (1998), Daly (1999), Nielsen and Jovicic (1999), Nuzzolo et al. (2001), Poon et al. (2004). The methods they proposed are collectively known as the schedule-based approach (Wilson and Nuzzolo, 2009).

Following the schedule-based approach, a number of researchers developed some mature assignment methods for networks whose links possess the PC and ACTS properties (for example, Hamdouch and Lawphongpanich, 2008; Sumalee et al., 2009; Papola et al., 2009; Nuzzolo et al., 2012). However, most of these models were designed for urban bus transport networks. We argue that bus transport networks significantly differ from coastal liner service networks. For example, if the traffic volume in a coastal liner service network is greater than its capacity, the freight rate on the corresponding transport channel may increase. Therefore, most of these assignment methods are not applicable to coastal liner service networks. We might say that there is no appropriate assignment method available that considers not only the PC and ACTS, but also some other specific features of coastal liner service networks (such as freight rate increment).

2.2. Related studies about liner route design

Ronen (1983, 1993) and Christiansen et al. (2004) systematically reviewed the studies on liner network design that were published before 2003. They divided liner network design into three sub-problems: fleet deployment, ship routing and scheduling. Early academic work focused on fleet deployment (Lane et al., 1987; Claessens, 1987; Jaramillo and Perakis, 1991; Perakis and Jaramillo, 1991; Rana and Vickson, 1991; Powell and Perkins, 1997). However, with the increment of the ports of call on a liner route, the quality of the route structure became a crucial factor influencing the operating cost. Thus, ship routing began to receive more attention, and many researchers turned to find methods to optimize ship routing and fleet deployment (or scheduling) simultaneously.

For example, Rana and Vickson (1988) presented an integer liner model to optimize the fleet size together with the liner-shipping route. Cho and Perakis (1996) adopted a set-partitioning model to optimize jointly fleet deployment and ship routing with the objective of maximizing revenue. Other researchers in this field include Fagerholt (1999, 2004) and Sambracos et al. (2004). Recently, a few researchers attempted to optimize the problems of ship routing, fleet deployment and scheduling simultaneously, for example, Agarwal and Ergun (2008) and Yan et al. (2009) provide a mixed-integer model to optimize ship scheduling and fleet deployment (or container shipment) together.

In addition, attempts have been made to incorporate some other factors into the liner ship routing problem. These factors include inventory management (Hsu and Hsieh, 2007), empty container relocation (Shintani et al., 2007; Liu et al., 2011; Dong and Song, 2009; Meng and Wang, 2011a,b), and seasonal fluctuations in transport demand (Meng and Wang, 2010).

Generally speaking, most of the above studies share the following common features: (a) The role of state subsidies or carbon emission reduction targets are not considered; (b) Most of these methods do not consider the influence of traffic assignment on liner route design.

To our knowledge, until now there are only two studies considering not only the influence of traffic assignment but also the role of state subsidies in the design of a transport network. Yamada et al. (2009) utilized the UE model when studying the coastal liner and inland transport network design problem. They first introduced a special impedance function applicable for waterway, highway and railway links, and then developed a bi-level programming model. The model can select a suitable set of actions from a set of alternatives (such as opening a shipping line, building ports or adding new railways), with the objective of maximizing the social benefit linked to a governmental investment.

Meng and Wang (2011a,b) developed a "mathematical program model with equilibrium constraints" for the intermodal hub-and-spoke network design problem. The model enables to locate hubs and sets highway, waterway and railway corridors with the objective of minimizing the total transport cost. The method also includes the UE model to estimate the traffic flow pattern, and defines an impedance function applicable for all the links. However, the methods proposed by the two

papers do not consider an optimization of the sequence of the ports of call. Moreover, the used impedance functions are unable to reflect the differences between highway links and waterway links as highlighted in the introductory sections of this paper.

3. Temporal–spatial expansion of the transport network and definition of the link impedance functions

In this section, we present essential building blocks for the specification of the New Coastal Liner Route Design Model (NCLRDM) by developing a mathematical expression for an intermodal transport network, and by explaining the Temporal–Spatial Expansion. Finally, we determine the impedance functions for the highway and waterway links respectively.

3.1. Mathematical description of the intermodal transport network

The intermodal transport network in a coastal area consists of the highway network and coastal liner routes. In this paper, we assume a bimodal system (trucking and coastal shipping). The railway network or river barge network is not considered. We use $\boldsymbol{G}_{cp} = (\boldsymbol{N}_c \cup \boldsymbol{N}_p, \boldsymbol{A}_{cp})$ representing the highway network that connects all coastal and inland cities and ports. Here $\boldsymbol{N}_c$ and $\boldsymbol{N}_p$ are the sets of cities and ports respectively; $\boldsymbol{A}_{cp}$ is the set of highway links. Besides, we use n_c and n_p representing the number of cities and ports respectively.

The description of the coastal liner routes is more complicated. The description of a given shipping route requires the following data inputs: the route service frequency, the ships deployed and the structure of the forward and backward sub-route in terms of port of call pattern. The last input is critical as it represents the skeleton of a shipping route. For instance, a forward sub-route configuration of "Port 1–Port 4–Port 7–Port 2" and a backward sub-route pattern equal to "Port 2–Port 3–Port 7–Port 1" allows specifying the entire structure of the liner-shipping route as shown in Fig. 1. Thus, the mathematical description should not only contain information about the nodes and links, but also about the forward sub-route, the backward sub-route, service frequency and ships deployed.

We use $\overline{\boldsymbol{G}}_k = (\overline{\boldsymbol{N}}_k, \overline{\boldsymbol{A}}_k, \overline{\boldsymbol{O}}_k^f, \overline{\boldsymbol{O}}_k^b, \bar{t}_k, \bar{f}_k)$ representing coastal liner route scheme k, where $\overline{\boldsymbol{N}}_k$ and $\overline{\boldsymbol{A}}_k$ are the sets of the ports of call and waterway links respectively; $\bar{t}_k$ is the ship type; $\bar{f}_k$ is the service frequency. $\overline{\boldsymbol{O}}_k^f$ and $\overline{\boldsymbol{O}}_k^b$ are the two ranges of integers representing the forward and backward sub-routes respectively. For instance, according to the case in Fig. 1, $\overline{\boldsymbol{O}}_k^f$ is {1, 4, 7, 2}; $\overline{\boldsymbol{O}}_k^b$ is {2, 3, 7, 1}. In addition, we use Ω representing the set of all feasible coastal liner routes.

If a coastal liner route $\overline{\boldsymbol{G}}_k$ is given, the intermodal network formed by $\boldsymbol{G}_{cp}$ and $\overline{\boldsymbol{G}}_k$ can be defined as $\widetilde{\boldsymbol{G}}_k = (\widetilde{\boldsymbol{N}}_k, \widetilde{\boldsymbol{A}}_k, \bar{t}_k, \bar{f}_k)$, where $\widetilde{\boldsymbol{N}}_k = \boldsymbol{N}_c \cup \boldsymbol{N}_p \cup \overline{\boldsymbol{N}}_k$, $\widetilde{\boldsymbol{A}}_k = \boldsymbol{A}_{cp} \cup \overline{\boldsymbol{A}}_k$ and $\boldsymbol{A}_{cp} \cap \overline{\boldsymbol{A}}_k = \phi$.

3.2. Temporal–spatial expansion of the intermodal network

We use a simple case to explain the temporal–spatial expansion and the way of expanding an intermodal network. Fig. 2 shows an intermodal network $\widetilde{\boldsymbol{G}}_k$, which involves two ports (Port 1 and Port 2), and two cities (City 3 and City 4). We assume that the highway transport time between Port 1 and City 3 is 6 h, the same as between Port 2 and City 4. The highway transport time between City 3 and City 4 is 72 h. We further assume that there is a liner shipping route between Port 1 and Port 2. On this route, a ship departs from Port 1 at 24h00 every day and arrives in Port 2 at 6h00. After 6 hours' intervals, the ship sails again and returns to Port 1 at 18h00.

The expanding process of the network is as follows:

Step 1: Establish a three-dimensional (3-D) space: By introducing the time dimension, we transform the two-dimensional (2-D) plane (Fig. 3a) to a 3-D space (Fig. 3b). In this 3-D space, the node can be denoted as a vector (x_i, y_i, tp), which represents City i (or Port i) at the time point tp. Here, the (x_i, y_i) is the plane coordinate of City i (or Port i). Then, Port 1 at 6h00 can be represented by the node $(x_1, y_1, 6)$ in Fig. 3b. We use $\widetilde{\boldsymbol{N}}$ representing the set of these nodes.

Step 2: Add directed links into the 3-D space based on the intermodal network: This step requires the completion of the following four sub-steps.

Sub-Step 2.1: Add directed links according to the highway transport time from cities to ports: In Fig. 2, the cargo flows starting from City 3 at 24h00 will arrive at Port 1 at 6h00. Thus, a directed link ***L1*** from node $(x_3, y_3, 0)$ to node $(x_1, y_1, 6)$ is inserted. As cargo flows starting from City 4 at 18h00 will arrive at Port 2 at 24h00 the next day, a directed link ***L2*** from node $(x_4, y_4, 18)$ to node $(x_2, y_2, 0)$ is add. By doing so, all links like ***L1*** and ***L2*** (the unidirectional links

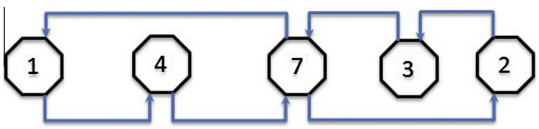

Fig. 1. Example of a route structure.

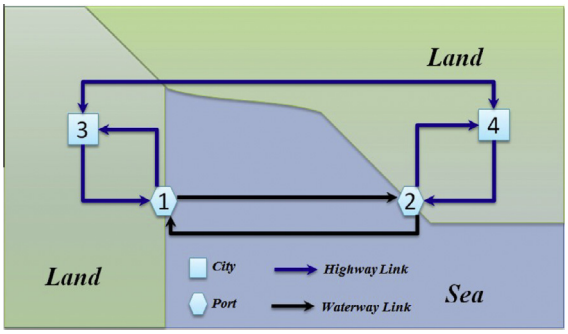

Fig. 2. Example of an intermodal network.

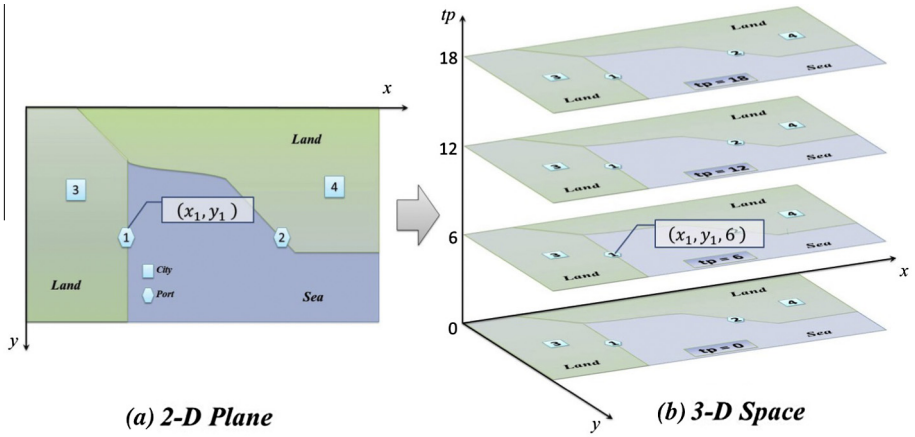

Fig. 3. Temporal–spatial expansion.

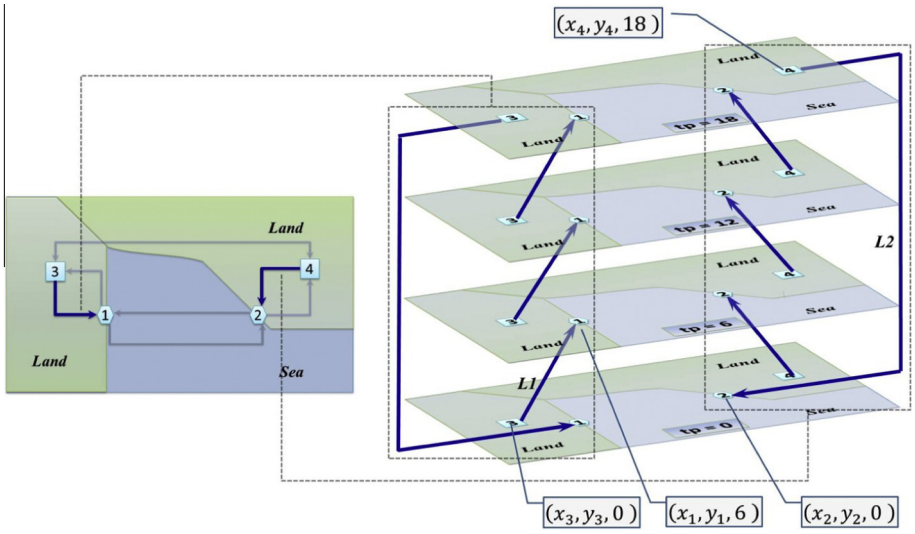

Fig. 4. Highway link from a city to a port.

represented by bold lines with arrowhead in Fig. 4) can be depicted in the 3-D space. These links are called "*highway link from city to port*". They are represented by set $\breve{\boldsymbol{A}}^1_{cp}$.

Sub-Step 2.2: Add directed links based on highway transport time from ports to cities: Following the method described in *Sub-Step 2.1*, we add directed links from ports to cities (the unidirectional links represented by bold lines with arrow heads in Fig. 5). Such links are called "*highway link from port to city*", and they are represented by set $\breve{\boldsymbol{A}}^2_{cp}$.

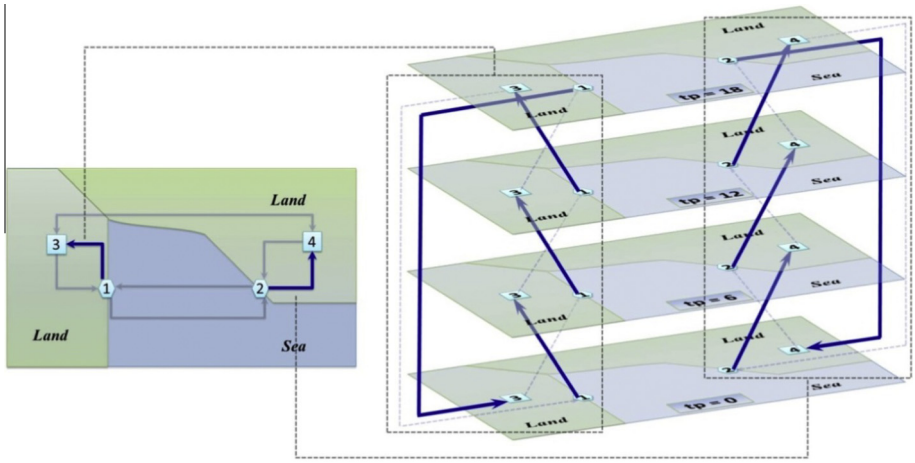

Fig. 5. Highway link from a port to a city.

Sub-Step 2.3: Add directed links based on the highway transport time between cities: In Fig. 2 the highway transport time between City 3 and City 4 is 72 h meaning that the cargo leaving City 3 by truck at 24h00 will arrive at City 4 three days later at 24h00. Accordingly, the directed link ***L3*** from node $(x_3,y_3,0)$ to node $(x_4,y_4,0)$ is inserted into the 3-D space. The directed link ***L4*** from node $(x_4,y_4,0)$ to node $(x_3,y_3,0)$ is inserted as well. As shown in Fig. 6, the bidirectional links are denotes as ***L3*** and ***L4***. These bidirectional links are referred as "*highway link between cities*", and the set of these links is $\breve{\boldsymbol{A}}^3_{cp}$.

Sub-Step 2.4: Add directed links according to the liner shipping route: In Fig. 2 the ship departures from Port 1 at 24h00 and arrives at Port 2 at 18h00 every day. Thus a directed link ***L5*** (in Fig. 7) is added from node $(x_1,y_1,0)$ to node $(x_2,y_2,6)$. The directed line ***L6*** is also inserted into the 3-D space. The set of these "*shipping*" links is $\breve{\boldsymbol{A}}^1_k$.

Sub-Step 2.5: As the ship is berthed at Port 1 from 18h00 to 24h00, it is necessary to add a directed link ***L7*** from node $(x_1,y_1,18)$ to node $(x_1,y_1,0)$ and the link ***L8*** from node $(x_2,y_2,6)$ to node $(x_2,y_2,12)$. This set of "*waiting links*" is represented by $\breve{\boldsymbol{A}}^2_k$.

Step 3: Add a dummy node and some dummy links for each city: In practice, cargo owners can decide on the departure time based on the available intermodal network. To reflect this phenomenon accurately, we set a dummy node for each city as the origin or destination of the cargo, and add some links to connect the dummy node to the 3-D network. For example, in Fig. 9 we created a dummy node VP_3 for City 3, and connected this node to the 3-D network by the dummy directed links ***L9*** to ***L12.*** The sets of dummy nodes and dummy links are denoted by $\breve{\boldsymbol{N}}_v$, and $\breve{\boldsymbol{A}}_v$ respectively.

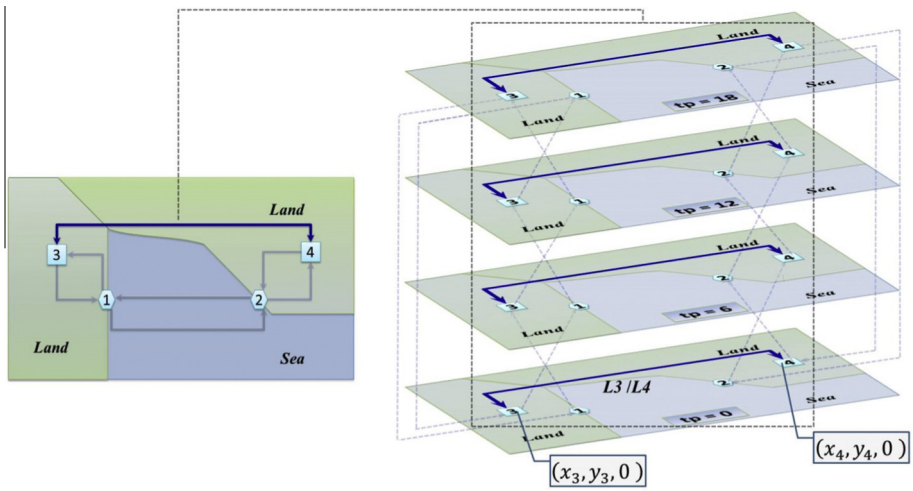

Fig. 6. Highway link between the cities.

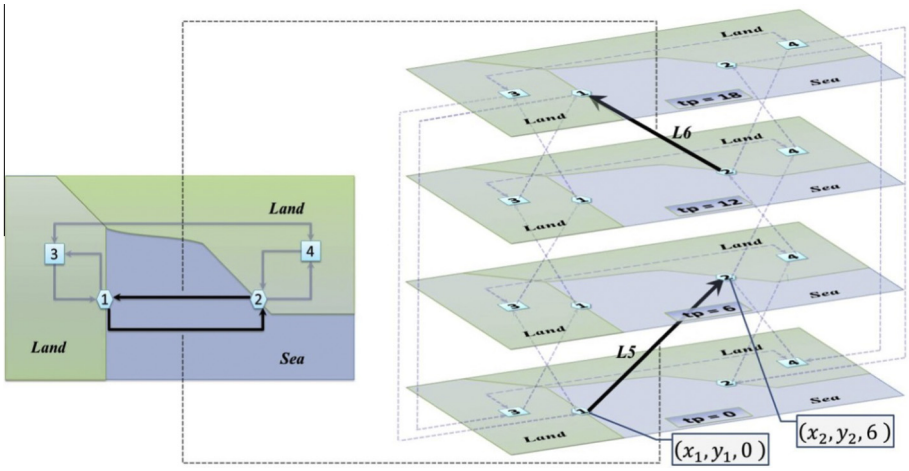

Fig. 7. Shipping links.

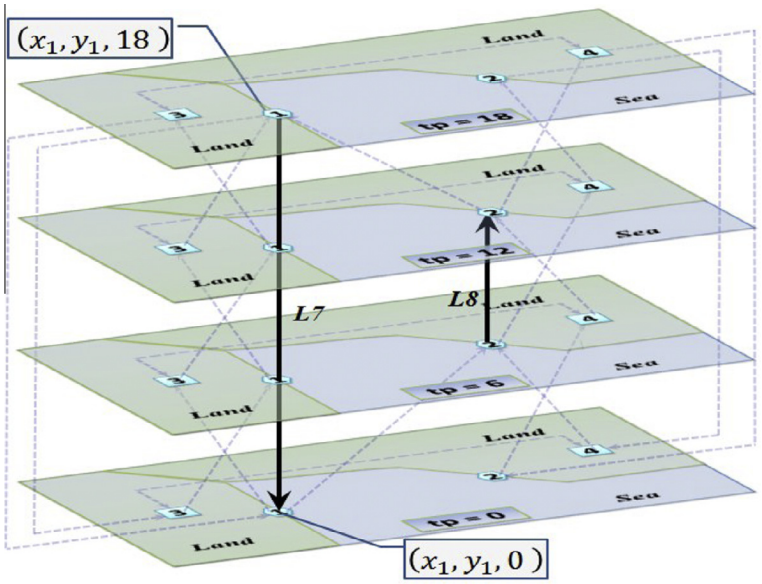

Fig. 8. Waiting links.

By following the above steps, a temporal–spatial network ($\widehat{\boldsymbol{G}}_k = (\widehat{\boldsymbol{N}}_k, \widehat{\boldsymbol{A}}_k)$) is created as shown in Fig. 10. Here the node set is denoted by $\widehat{\boldsymbol{N}}_k = \breve{\boldsymbol{N}} \cup \breve{\boldsymbol{N}}_v$ and the link set is denoted by $\widehat{\boldsymbol{A}}_k = \breve{\boldsymbol{A}}^1_{cp} \cup \breve{\boldsymbol{A}}^2_{cp} \cup \breve{\boldsymbol{A}}^3_{cp} \cup \breve{\boldsymbol{A}}^1_k \cup \breve{\boldsymbol{A}}^2_k \cup \breve{\boldsymbol{A}}_v$. In the following sections, we use function $\widehat{\boldsymbol{G}}_k = g_{ex}(\widetilde{\boldsymbol{G}}_k)$ as expression for the temporal–spatial expansion.

In the 3-D network $\widehat{\boldsymbol{G}}_k$, it is possible to describe any feasible cargo transport scheme by a path. For example, the path described by the bold red directed links in Fig. 10 represents the following transport scheme. The cargo leaves City 4 at 6h00 by truck and arrives at Port 2 some 6 h later. After a modal change to maritime transport, Port 1 is reached at 18h00. After arriving in Port 1, the cargo moves by truck to arrive in City 4 at 24h00 the next day. In this temporal–spatial network, no link shows the PC property. Besides, it should be noted that Figs. 3–10 present merely some sketches. In the calculation section, we actually set 24 layers (one layer per hour).

We introduce the concept of "*map*" to describe the relationship between a link in $\widetilde{\boldsymbol{G}}_k$ and the corresponding one in $\widehat{\boldsymbol{G}}_k$.

Definition. Supposing a: $(x_i, y_i) - (x_j, y_j)$ is a link in $\widetilde{\boldsymbol{G}}_k$, $\hat{a} : (\hat{x}_i, \hat{y}_i, tp_i) - (\hat{x}_j, \hat{y}_j, tp_j)$ is a link in $\widehat{\boldsymbol{G}}_k$, if $\widehat{\boldsymbol{G}}_k = g_{ex}(\widetilde{\boldsymbol{G}}_k)$, $x_i = \hat{x}_i$, $x_j = \hat{x}_j$, $y_i = \hat{y}_i$, $y_j = \hat{y}_j$, then we say that link $\hat{a}$ *maps* link a, written as $\hat{a} = g_{map}(a, \widetilde{\boldsymbol{G}}_k)$. When $\hat{a} = g_{map}(a, \widetilde{\boldsymbol{G}}_k)$, the length of $\hat{a}$ (denoted by $D_{\hat{a}}$) equals the length of a(D_a), the travel time of $\hat{a}$ (denoted by $t_{\hat{a}}$) equals the travel time of a (denoted by t_a). These two relations can be expressed as follows:

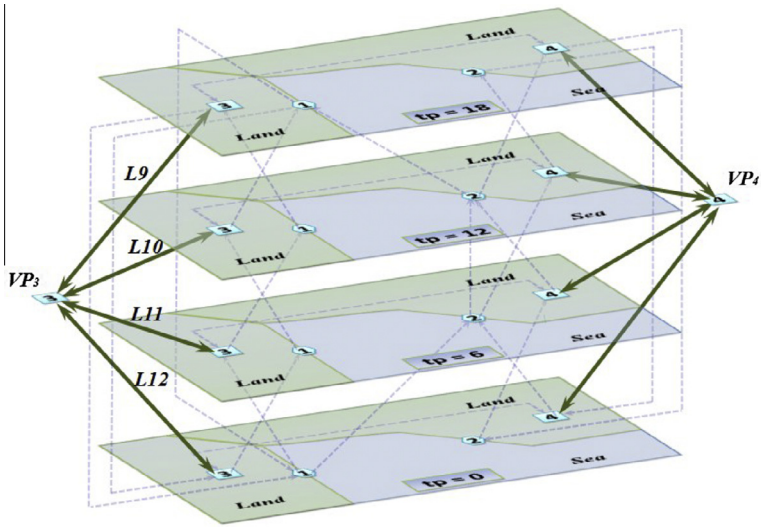

Fig. 9. Dummy links.

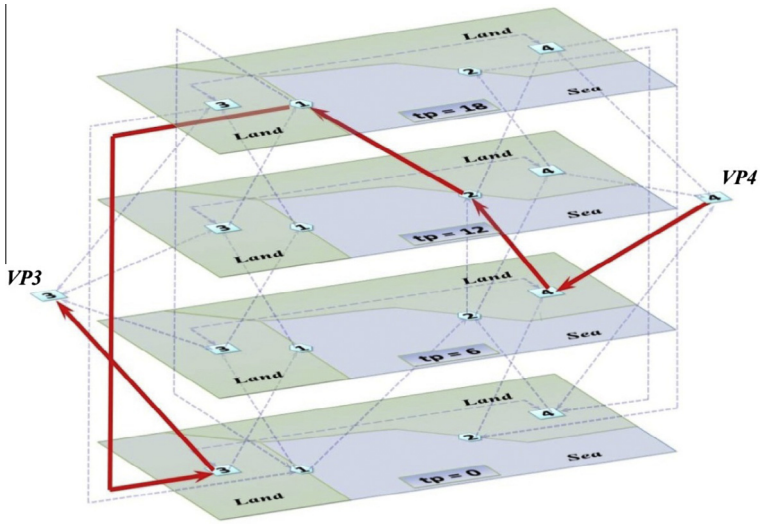

Fig. 10. A feasible cargo transport scheme.

$$t_{\hat{a}} = t_a \quad \hat{a} \in \breve{\boldsymbol{A}}^1_{cp} \cup \breve{\boldsymbol{A}}^2_{cp} \cup \breve{\boldsymbol{A}}^3_{cp} \cup \breve{\boldsymbol{A}}^1_{k}, a \in \overline{\boldsymbol{A}}_k, \quad \hat{a} = g_{map}(a, \widetilde{\boldsymbol{G}}_k) \tag{1}$$

$$D_{\hat{a}} = D_a \quad \hat{a} \in \breve{\boldsymbol{A}}^1_{cp} \cup \breve{\boldsymbol{A}}^2_{cp} \cup \breve{\boldsymbol{A}}^3_{cp} \cup \breve{\boldsymbol{A}}^1_{k}, a \in \overline{\boldsymbol{A}}_k, \quad \hat{a} = g_{map}(a, \widetilde{\boldsymbol{G}}_k) \tag{2}$$

3.3. Determination of the impedance functions

3.3.1. Impedance function of highway links

The impedance function is used to calculate the generalized cost incurred by cargo owners when their cargos pass through a transport link. According to Meng and Wang (2011a,b), the impedance function of highway links can be expressed as the sum of the actual freight cost and the value of the transport time. Thus, the impedance function of a highway link can be defined as follows:

$$u_{\hat{a}}(z_{\hat{a}}) = p^{cp}_{\hat{a}} + \mu \cdot t_{\hat{a}} \qquad \hat{a} \in \breve{\boldsymbol{A}}^1_{cp} \cup \breve{\boldsymbol{A}}^2_{cp} \cup \breve{\boldsymbol{A}}^3_{cp} \tag{3}$$

Here, $\hat{a}$ represents a link in temporal–spatial network $\widehat{\boldsymbol{G}}_k$; $z_{\hat{a}}$ denotes the traffic volume on link $\hat{a}$; $t_{\hat{a}}$ is the transport time; μ is the value of time (VOT). $p^{cp}_{\hat{a}}$ is the unit price of highway transport by truck. In this paper, we assume $p^{cp}_{\hat{a}}$ is constant. At

present, the capacity of highway systems in China is far beyond actual demand with only very few exceptions (mainly in the urban areas of major coastal cities such as Shanghai). This makes the Chinese highway system seldom incur congestion. Therefore, we do not consider the question of congestion on highway links.

3.3.2. Impedance functions of shipping and waiting links

For determining the impedance functions of shipping and waiting links, we consider two things: (a) the ACTS; and (b) the interaction between the unit price of maritime transport and the traffic volume. The impedance function of the shipping link is defined as follow:

$$u_{\hat{a}}(z_{\hat{a}}) = \begin{cases} p_{\hat{a}}^k + \mu \cdot t_{\hat{a}} & z_{\hat{a}} \leqslant C_k \\ \overline{M} \cdot (C_k - z_{\hat{a}})^2 + p_{\hat{a}}^k + \mu \cdot t_{\hat{a}} & z_{\hat{a}} > C_k \end{cases} \quad \hat{a} \in \breve{\boldsymbol{A}}_k^1 \tag{4}$$

$$p_{\hat{a}}^k = c_{\hat{a}} \cdot [1 + \alpha_1 (z_{\hat{a}}/C_k)^{\alpha_2}] \tag{5}$$

Here, $\overline{M}$ is a big enough constant; $p_{\hat{a}}^k$ is the unit transport price of link $\hat{a}$; C_k is the capacity of the ship type $\bar{t}_k$; $c_{\hat{a}}(\hat{a} \in \breve{\boldsymbol{A}}_k^1)$ is the operating cost of shipping link $\hat{a}$; and α_1 and α_2 are the parameters.

Eq. (4) shows the impedance function of a shipping link. It means that if $z_{\hat{a}}$ is smaller than C_k, $u_{\hat{a}}(z_{\hat{a}})$ will equal a number: $p_{\hat{a}}^k + \mu \cdot t_{\hat{a}}$; Otherwise, it will equal a large number: $\overline{M} \cdot (C_k - z_{\hat{a}})^2 + p_{\hat{a}}^k + \mu \cdot t_{\hat{a}}$. Eq. (4) ensures the being carried cargos cannot be greater than the capacity of the link. Here we suppose that there is a relationship (Eq. (5)) among the traffic volume, the unit shipping price and the shipping capacity. Specially, we assume that the unit coastal shipping price depends on the ratio between traffic volume and link capacity. When the ratio is near to unity, the operator will raise the price.

Based on Eq. (4), the impedance function of a waiting link can be expressed as follows:

$$u_{\hat{a}}(z_{\hat{a}}) = \begin{cases} \mu \cdot t_{\hat{a}} & z_{\hat{a}} \leqslant C_k \\ \overline{M} \cdot (C_k - z_{\hat{a}})^2 + \mu \cdot t_{\hat{a}} & z_{\hat{a}} > C_k \end{cases} \quad \hat{a} \in \breve{\boldsymbol{A}}_k^2 \tag{6}$$

Unlike the shipping link, there is no need to consider the unit-shipping price in the impedance function of the waiting link.

3.3.3. Impedance function of dummy links

As there is no capacity limitation for dummy links and cargo can pass through these links without any time or monetary implications, the impedance function of all dummy links is always 0 (Eq. (7)).

$$u_{\hat{a}}(z_{\hat{a}}) = 0 \qquad \hat{a} \in \breve{\boldsymbol{A}}_v \tag{7}$$

The above impedance functions are all monotonic and differentiable. They satisfy the conditions required by the UE model allowing us to use the Beckman model (Sheffi, 1984) to obtain the UE traffic flows on the temporal–spatial network. In the next section, we establish the NCLRDM based on these impedance functions and the temporal–spatial expansion.

4. Model structure

4.1. General specification of NCLRDM

The NCLRDM is a bi-level programming model that consists of two sub-models (Fig. 11). One sub-model is an integer-programming model (UPPER model). It selects the best liner route scheme from the feasible set Ω with the objective of minimizing state subsidies, and under the conditions of realizing the goals of bringing a reasonable profit to the liner operators and reducing carbon emissions.

The other one (LOWER model) is the UE assignment model (the Beckman Transformation). The LOWER model has four roles (Fig. 11):

(a) to combine a given $\overline{\boldsymbol{G}}_k$ with $\boldsymbol{G}_{cp}$ to create an intermodal network $\widetilde{\boldsymbol{G}}_k$, and expanding $\widetilde{\boldsymbol{G}}_k$ to the temporal–spatial network $\widehat{\boldsymbol{G}}_k$;
(b) to assign the OD traffic on $\widehat{\boldsymbol{G}}_k$;
(c) to estimate the carbon emission and the profit of $\overline{\boldsymbol{G}}_k$; and
(d) to return the results to the UPPER model as the evaluating criteria for $\overline{\boldsymbol{G}}_k$.

Next, we will discuss the UPPER and LOWER models in more detail.

4.2. Specification of the UPPER model

The UPPER model is described as follows:

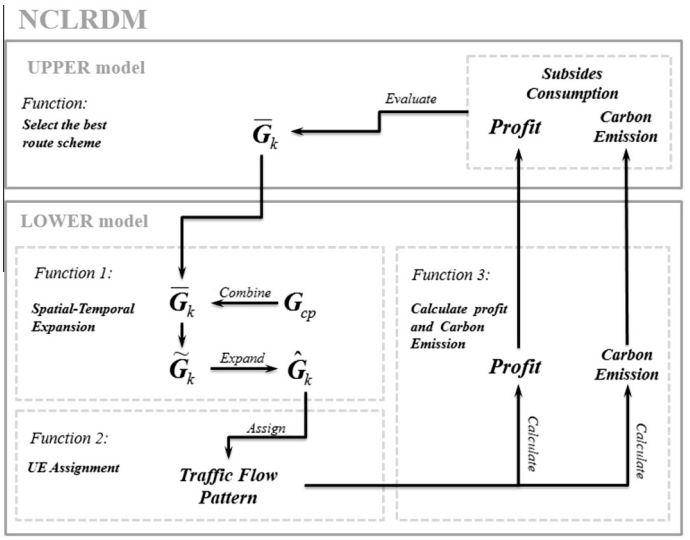

Fig. 11. The structure of the NCLRDM.

$$\textbf{Min}: Obj_U = \sum_k \rho_k [r_p \cdot g_c(\overline{\boldsymbol{G}}_k) - g_p(\overline{\boldsymbol{G}}_k)] \tag{8}$$

$$\boldsymbol{S.T.}: \sum_{\overline{\boldsymbol{G}}_k \in \Omega} \rho_k = 1 \tag{9}$$

$$\rho_k = \begin{cases} 1 & \text{if shipping route } k \text{ is selected} \\ 0 & \text{otherwise} \end{cases} \quad \forall \overline{\boldsymbol{G}}_k \in \Omega \tag{10}$$

$$t_a = D_a / v_L \qquad a \in \boldsymbol{A}_{cp} \tag{11}$$

$$t_a = D_a / v_k \qquad a \in \overline{\boldsymbol{A}}_k \tag{12}$$

$$n_{ship} = g_{ceil}\left(\sum_{a \in \overline{\boldsymbol{A}}_k} (t_a + t_{berth} \cdot n_{pk}) \times \bar{f}_k / 24\right) \tag{13}$$

$$c_a^k = \frac{t_a}{\sum_{b \in \overline{\boldsymbol{A}}_k} t_b} \cdot \frac{p_k^{rent} \cdot n_{ship}}{C_k} \; a \in \overline{\boldsymbol{A}}_k \tag{14}$$

$$g_c(\overline{\boldsymbol{G}}_k) = \sum_{a \in \overline{\boldsymbol{A}}_k} c_a^k \cdot C_k \tag{15}$$

$$r_k^{em} = (E_o - \bar{e}_k)/E_o \tag{16}$$

$$r_k^{em} \geqslant R_{ex}^{em} \tag{17}$$

where $\overline{\boldsymbol{G}}_k = (\overline{\boldsymbol{N}}_k, \overline{\boldsymbol{A}}_k, \overline{\boldsymbol{O}}_k^f, \overline{\boldsymbol{O}}_k^b, \bar{\boldsymbol{t}}_k, \bar{\boldsymbol{f}}_k) \overline{\boldsymbol{G}}_k \in \Omega$.

The objective function (Eq. (8)) minimizes the state subsidy which would be required to guarantee an acceptable rate of return to the operator, which is at least not lower than the operator's expectation (r_p). In Eq. (8), ρ_k is a decision variable, if $\overline{\boldsymbol{G}}_k$ is selected, ρ_k is 1, otherwise it is 0 (Eq. (10)); $g_c(\overline{\boldsymbol{G}}_k)$ is the operating cost of $\overline{\boldsymbol{G}}_k$. The operator's profit from $\overline{\boldsymbol{G}}_k$ is represented by $g_p(\overline{\boldsymbol{G}}_k)$, which is obtained from the LOWER model.

It should be noted that Obj_U can be either positive or negative. A positive Obj_U means government should provide subsidies to the operator. While a negative one implies the operator will earn enough profit as well as achieve the emission reduction goal. At this point, there is no need for the government to provide subsidies.

In the constraints section of the mathematical expressions, v_k represents the speed of the ship adopted by $\overline{\boldsymbol{G}}_k$; v_L is the average speed of trucks using the highways; n_{ship} is the ship number required for operating $\overline{\boldsymbol{G}}_k$; $g_{ceil}(\cdot)$ is a ceiling function, which returns the nearest integer greater than or equal to the element between brackets; n_{pk} represents the number of the ports of call in $\overline{\boldsymbol{G}}_k$; t_{berth} is the berthing time of the ships at each port, here t_{berth} is assumed as a constant; c_a^k is the unit operating cost of link a ($a \in \overline{\boldsymbol{A}}_k$); p_k^{rent} is the daily charter cost of each ship. E_o and $\bar{e}_k$ represent the carbon emissions before and after the implementation of $\overline{\boldsymbol{G}}_k$ respectively; r_k^{em} is the carbon-reduction rate; R_{ex}^{em} is the minimum carbon-reduction rate expected by the government.

Eq. (9) ensures that only one route scheme can be selected. Eqs. (11) and (12) calculate the transport times on the highway and shipping links respectively. Eq. (13) calculates the number of the ships needed by $\overline{\boldsymbol{G}}_k$. Eq. (14) calculates c_a^k. Eq. (15) calculates $g_c(\overline{\boldsymbol{G}}_k)$. Eq. (16) computes r_k^{em}, in which $\bar{e}_k$ is obtained from the LOWER model. Eq. (17) ensures that the selected $\overline{\boldsymbol{G}}_k$ can realize the R_{ex}^{em} goal.

4.3. Specification of the LOWER model

The LOWER model can be written as follows:

$$\textbf{Min}: Obj_L = \sum\nolimits_{\hat{a}\in\widehat{\boldsymbol{A}}_k} \int_0^{z_{\hat{a}}} \mu_{\hat{a}}(\omega)d\omega \tag{18}$$

$$\textbf{S.T.}: \widehat{\boldsymbol{G}}_k = g_{ex}(\widetilde{\boldsymbol{G}}_k) \tag{19}$$

$$q_{ij} = \sum\nolimits_b s_{ijb} \quad i,j \in \widehat{\boldsymbol{N}}_k \tag{20}$$

$$z_{\hat{a}} = \sum\nolimits_i \sum\nolimits_j \sum\nolimits_b s_{ijb}\cdot\sigma_{ijab} \qquad \hat{a}\in\widehat{\boldsymbol{A}}_k \tag{21}$$

$$c_{\hat{a}} = c_a^k \quad \hat{a}\in\breve{\boldsymbol{A}}_k^1, \quad \hat{a} = g_{map}(a,\widetilde{\boldsymbol{G}}_k) \quad a\in\overline{\boldsymbol{A}}_k \tag{22}$$

$$p_{\hat{a}}^{cp} = p_a^{cp} \qquad \hat{a}\in\breve{\boldsymbol{A}}_{cp}^1\cup\breve{\boldsymbol{A}}_{cp}^2\cup\breve{\boldsymbol{A}}_{cp}^3, \hat{a} = g_{map}(a,\boldsymbol{G}_{cp}), a\in\boldsymbol{A}_{cp} \tag{23}$$

$$g_p(\overline{\boldsymbol{G}}_k) = \sum\nolimits_{\hat{a}\in\breve{\boldsymbol{A}}_k^1}[p_{\hat{a}}^k\cdot z_{\hat{a}} - c_{\hat{a}}\cdot C_k] \tag{24}$$

$$\bar{e}_k = \sum\nolimits_{\hat{a}\in\breve{\boldsymbol{A}}_k^1} C_k\cdot e_s\cdot D_{\hat{a}} + \sum\nolimits_{\hat{a}\in\breve{\boldsymbol{A}}_{cp}^1\cup\breve{\boldsymbol{A}}_{cp}^2\cup\breve{\boldsymbol{A}}_{cp}^3} z_{\hat{a}}\cdot e_l\cdot D_{\hat{a}} \tag{25}$$

where $z_{\hat{a}}, s_{ijb} \geqslant 0$.

Eq. (18) is the objective function, which constitutes a Beckmann transfer together with Eqs. (19) and (20). Here, $z_{\hat{a}}$ is the traffic flow of link $\hat{a}$ in the temporal–spatial network $\widehat{\boldsymbol{G}}_k$ (acquired from Eq. (19)); q_{ij} is the known transport demand from origin node i to destination node j in $\widehat{\boldsymbol{G}}_k$; s_{ijb} is the traffic flow on path b connecting an origin–destination (OD) pair i–j; σ_{ijab} is an indicator variable, if link $\hat{a}$ is on path b between OD pair i–j, it is 1, otherwise 0. The impedance function $\mu_{\hat{a}}(\cdot)$ has already been defined by Eqs. (3)–(7). Some of the parameters in the impedance functions are calculated by Eqs. (1), (2), and (22) and Eqs. (23) and (24) calculates $g_p(\overline{\boldsymbol{G}}_k)$. Eq. (25) calculates $\bar{e}_k$, where e_s and e_l are the emission factors of the maritime/water transport and highway transport respectively.

5. Model solution

5.1. Genetic and Frank–Wolfe Hybrid Algorithm (GFWHA)

We propose a Genetic and Frank–Wolfe Hybrid Algorithm (GFWHA) to solve the NCLRDM. The process of the GFWHA is as follows:

Algorithm: GFWHA

Step 1 (Initialization)
Set $n = 0$, and create the initial population $Pop_n = \{\overline{\boldsymbol{G}}_{\boldsymbol{k}}^{\boldsymbol{n}} | \boldsymbol{k} = \boldsymbol{1},\boldsymbol{2},\cdots,\lambda\}$, in which individual $\overline{\boldsymbol{G}}_k^n$ is the kth liner shipping route scheme in the nth generation, λ is the population size.

Step 2 (Calculate carbon-emission, and $\boldsymbol{Gs}_k^n$'s profit and operating cost)
For each $\overline{\boldsymbol{G}}_k^n$ of Pop_n:
Step 2.1 Calculate the operating cost $g_c(\overline{\boldsymbol{G}}_{\boldsymbol{k}}^{\boldsymbol{n}})$;
Step 2.2 Combine $\overline{\boldsymbol{G}}_k^n$ with $\boldsymbol{G}_{cp}$ to build intermodal network $\widetilde{\boldsymbol{G}}_k^n$;
Step 2.3 Expand $\widetilde{\boldsymbol{G}}_k^n$ to obtain temporal–spatial $\widehat{\boldsymbol{G}}_k^n$;
Step 2.4 Calculate the traffic flow $z_{\hat{a}}$ on link $\hat{a}$ according to $\widehat{\boldsymbol{G}}_k^n$ by Frank–Wolfe Algorithm;
Step 2.5 Calculate the carbon emission $\overline{e}_k^n$ and profit $g_p(\overline{\boldsymbol{G}}_{\boldsymbol{k}})$, based on $z_{\hat{a}}$, with Eqs. (24) and (25).

Step 3 (Calculate the fitness value of $\overline{\boldsymbol{G}}_k^n$)
For each $\overline{\boldsymbol{G}}_k^n$ of Pop_n, calculate the fitness value fit_k^n of $\overline{\boldsymbol{G}}_k^n$ based on $g_p(\overline{\boldsymbol{G}}_{\boldsymbol{k}}^{\boldsymbol{n}}), g_c(\overline{\boldsymbol{G}}_{\boldsymbol{k}}^{\boldsymbol{n}}), r_p, \overline{e}_k^n$ and E_o.

Step 4 (Implement selection, crossover and mutation)
Set $n = n + 1$. Implement selection, crossover and mutation according to fit_k^n, and finally obtain a new population Pop_n.

Step 5 (Judge whether to stop the calculation)
If $|max(fit_k^n) - average(fit_k^n)| \leqslant \xi$; (a given parameter) then
  Stop the calculation;
Else
  Go to step 2.

The GFWHA is developed from GA, so its performance is also largely influenced by the design of genetic operators and the value of the parameters (such as the size of population, the rates of crossover and mutation, and so on). When designing the GFWHA, we firstly pre-determined several alternative schemes about the genetic operators and parameters. Then, we made the calculations with these respective schemes and compared the results. Finally, we selected the scheme that can improve the performance of the algorithm the most. For example, while designing the selection operator, we considered three alternative options: (a) using the roulette-wheel-selection operator; (b) using the tournament selection operator; (c) using both of them. In the end, we selected the third option: the tournament selection operator is used in the first one-third of the iteration process, and the roulette wheel selection operator is adopted in the flowing two-thirds. In the next sections, we explain three key elements of the GFWHA: the fitness function, the coding method and the crossover method.

5.2. Fitness function

The fitness function is as follow:

$$fit_k^n = -[r_p \cdot g_c(\overline{\boldsymbol{G}}_{\boldsymbol{k}}^{\boldsymbol{n}}) - g_p(\overline{\boldsymbol{G}}_{\boldsymbol{k}}^{\boldsymbol{n}})] - M \cdot \max(0, R_{ex}^{em} - \bar{e}_k^n) \tag{26}$$

$$M = [max(H_1, \cdots, H_n) - min(H_1, \cdots, H_n)] \times 0.3 \times [1 + 10 \times (R_{ex}^{em} - \bar{e}_k^n)^2] \tag{27}$$

$$H_n = -[r_p \cdot g_c(\overline{\boldsymbol{G}}_{\boldsymbol{k}}^{\boldsymbol{n}}) - g_p(\overline{\boldsymbol{G}}_{\boldsymbol{k}}^{\boldsymbol{n}})] \tag{28}$$

where $[r_p \cdot g_c(\overline{\boldsymbol{G}}_{\boldsymbol{k}}^{\boldsymbol{n}}) - g_p(\overline{\boldsymbol{G}}_{\boldsymbol{k}}^{\boldsymbol{n}})]$ calculates the required subsidy of $\overline{\boldsymbol{G}}_{\boldsymbol{k}}^{\boldsymbol{n}}$, and the penalty term $M \cdot \max(0, R_{ex}^{em} - \bar{e}_k^n)$ ensures that the algorithm picks out the $\overline{\boldsymbol{G}}_{\boldsymbol{k}}$s, which can realize the minimum carbon-reduction rate (R_{ex}^{em}) at least. It should be noted that the value of M is very important for the performance of the GFWHA. Here we use Eqs. (27) and (28) to calculate M. This method makes it possible for the GFWHA to adjust M according to changes of the population so to keep M in a reasonable interval.

5.3. Coding method

We modify the method of Yang et al. (2012) to code the chromosome to represent a shipping route scheme. Each chromosome has five parts (Fig. 12). Part 1 represents the ship type deployed on the route. Part 2 represents the service frequency. Parts 3–5 indicate the route structure. Part 3 represents the range of ports; Parts 4 and 5 respectively represent the ports of call on the forward sub-route and backward sub-route. If a port is on the route, the corresponding gene is 1, otherwise, it is 0. The forward call sequence is determined by the genes from left to right in Part 3 and the ports of call in Part 5. Similarly, the backward call sequence is decided by the genes from right to left in Part 3 and the ports of call in Part 3. For example, in Fig. 13 the genes in Part 3 from left to right are 61528374. Part 4 shows that the ports of call include 1347. Thus, the forward call sequence is 1374. The reverse order of Part 1 is 47382516. Part 3 shows that the ports of call are 12374. Thus, the backward call sequence is 47321.

5.4. Crossover method

We implement a crossover operation for the five parts of the chromosome. A Single-point Crossover Method is applied for Parts 1 and 2, a Generalized N-point Crossover Method (Surry et al., 1995) is used for Part 3, and a Two-point Crossover Method is adopted for Parts 4 and 5. It is possible that the crossover operation produces certain "problem chromosomes",

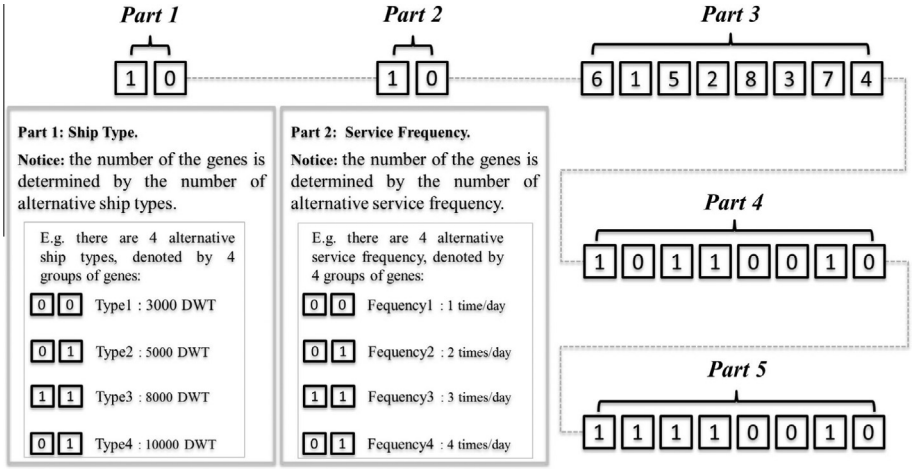

Fig. 12. Chromosome of the GAFWA.

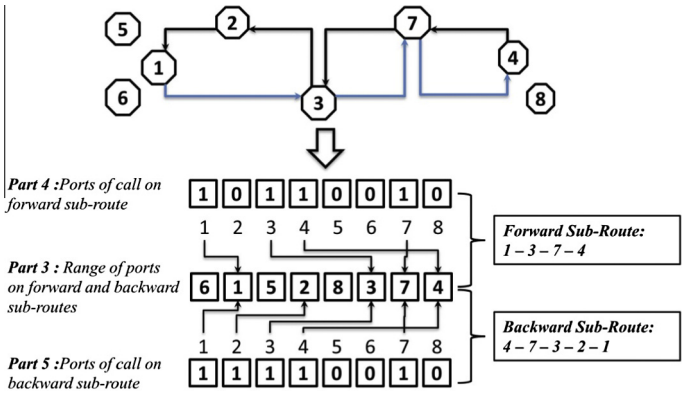

Fig. 13. Representation of the route structure.

which describes an unfeasible route structure. For example, it is possible to obtain a problem chromosome shown in Fig. 14. Here, Part 3 is 61548732, Part 4 is 01011001, and Part 5 is 10110010. At this point, the forward sub-route is 5482 and the backward sub-route is 3741. This chromosome represents an unfeasible shipping route scheme, as it is not possible to form a closed loop. The problem chromosomes can be corrected by the following method.

Correcting method for the problem chromosome (CMPC)

Step 1 Find the ports of call

Find all the ports of call indicated by Part 4 and Part 5. For example, the ports of call include Port 1234578 in the case of Fig. 14.

Step 2 Create a temporary range of the ports of call

Create a temporary range by sequencing the ports of call according to Part 3. The range will be used to correct Part 4 and Part 5. In Fig. 14, as Part 3 is 61548732, the temporary range is 1548732.

Step 3 Correct the forward sub-route and Part 4

First, compare the first port of call in the temporary range with the departure port of the forward sub-route. If they are different, add the first port of the range into the forward sub-route as the departure port. Second, compare the last port of the temporary range with the last port in the forward sub-route. Again, if they are different, add the last port of the range into the forward sub-route as the last port of call. Finally, correct Part 4 according to the revised forward sub-route.

In the case of Fig. 14, the first port (Port 1) of the temporary range (1548732) is different from the departure port (Port 5) of the forward sub-route (5482). Thus we add Port 1 into the forward sub-route as the departure port to create a new forward sub-route (15482), and change the corresponding gene (the 1st gene) in Part 4 into 1. Finally a corrected Part 4 (11011001) is obtained.

Step 4 Correct backward sub-route and Part 5

First, compare the last port of call in the temporary range with the departure port of the backward sub-route. If they are different, add the terminal port of the range into the backward sub-route as the departure port. Second, compare the first port of the temporary range with the last port of call in the backward sub-route. If they are different, add the departure port of the range into the backward sub-route as the last port. Finally, correct Part 5 according to the revised backward sub-route.

In the case of Fig. 15, the last port (Port 2) of the temporary range is different from the departure port (Port 3) of the backward sub-route (3741). Thus, port 2 is inserted into the backward sub-route as the departure port. Now the backward sub-route is corrected to 23741, and the 2nd gene of Part 5 is changed to 1. Finally a corrected Part 5 (1 1 1 1 0 0 1 0) is obtained.

6. Empirical application

6.1. Area description and data collection

In this section, we demonstrate the NCLRDM by applying the model to the coastal liner route design problem in the Bohai Bay region in the northeastern part of China (Fig. 15). The Bohai Bay region is one of the most important and cargo-rich multi-port gateway regions in China (see Notteboom, 2010 for terminology) next to the Pearl River Delta in southern China (including ports such as Hong Kong, Shenzhen, Guangzhou and Zhuhai) and the Yangtze River Delta (Shanghai, Ningbo, Taicang, Nanjing).

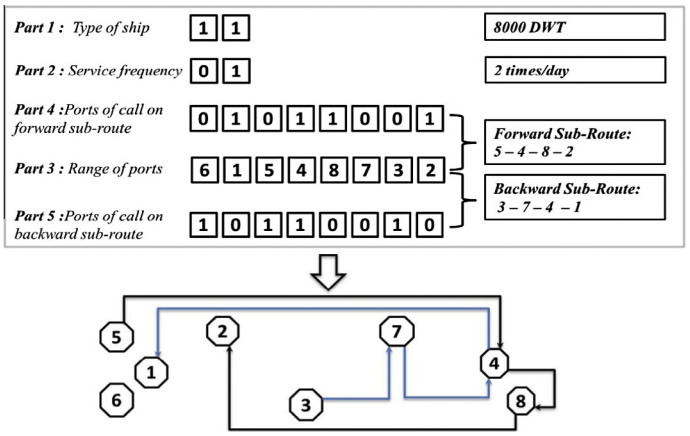

Fig. 14. The problem chromosome.

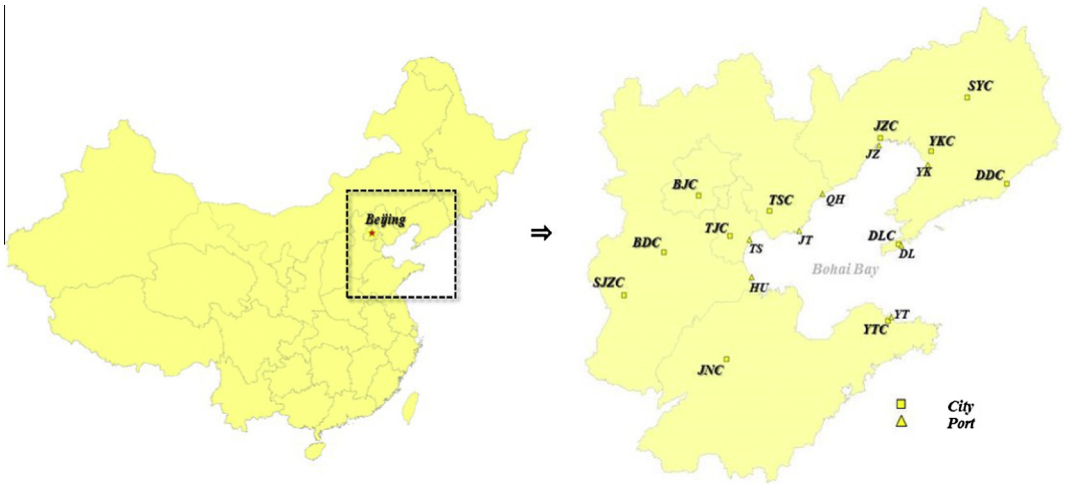

Fig. 15. The Western Bohai Bay region.

All major gateway ports in the Bohai Bay region are included in the empirical application: Yingkou (YK), Jinzhou (JZ), Qinhuangdao (QD), Jingtang (JT), Tianjin (TS), Huanghua (HU), Dalian (DL) and Yantai (YT) ports. The list of selected cities consists of Shenyang (SYC), Jinzhou (JZC), Yingkou (YKC), Tangshan (TSC), Tianjin (TJC), Beijing (BJC), Baoding (BDC), Shijiazhuang (SJZC), Jinan (JNC), Weihai (WHC), Dalian (DLC), Yantai (YTC), and Dandong (DDC). The OD traffic flows between these cities were obtained from a confidential report made by a Chinese local government (Table 1). The corresponding traffic flow patterns are depicted in Fig. 16.

The parameters related to highway transport are as follows: e_l = 289 g CO_2/ton km (Perakis and Denisis, 2008), $p_a^{cp} = 0.803$ CNY/ton km and $v_L = 70$ km/h.

The parameters related to waterway/maritime transport are: e_s = 35g CO_2/ton km (Perakis and Denisis, 2008), the alternative ship types have a deadweight capacity of 6000 DWT (Deadweight Tonnage), 8000 DWT, 14,000 DWT and 20,000 DWT. The respective vessel charter costs are calculated using Eq. (29). The respective sailing speeds are set at 18 kn, 18 kn, 20 kn and 22 kn. In addition, the alternative service frequencies include 1, 2, 3 and 4 sailings per day. The operator's lowest expected rate of return is 10%.

$$p_k^{rent} = 0.2066 \cdot C_k + 12,208 \tag{29}$$

The parameters related to the impedance functions: According Meng and Wang (2011a,b), we set α_1 = 1.113, α_2 = 3.048. The VOT of waterway links equals μ = 0.1 CNY/ton km h and the VOT of highway links is set at μ = 1.5 CNY/ton km h.

The parameters related to the GFWHA: The population size is 100; and the maximum number of iterations is 150; the mutation rate is 0.02; and the crossover rate is set at 0.80. The stopping threshold ξ is 0.01.

In addition, considering the GFWHA is a heuristic and its conclusions may not be convincing, we took the following measures to guarantee the reliability of the experiment results. First, for a given minimum carbon-reduction rate, we performed

Table 1
OD traffic flows between cities (in ton per day).

	DLC	DDC	SYC	JZC	YKC	TSC	TJC	BJC	BDC	SJZC	JNC	YTC
DLC	0	8219	21,918	2192	2192	10,959	16,438	21,918	2740	82,192	27,397	548
DDC	822	0	2740	822	548	2192	1096	2192	822	3288	3836	822
SYC	10,959	3288	0	1096	822	2740	35,616	57,534	8219	136986	82,192	8219
JZC	822	548	2192	0	548	1096	2740	6027	2192	10,959	3288	822
YKC	822	1096	5479	8219	0	10,959	5479	16,438	3836	54,795	5479	548
TSC	5479	3288	8219	2192	2740	0	8219	13,699	2192	13,699	16,438	822
TJC	21,918	5479	35,616	2192	3288	5479	0	82,192	5479	109589	164384	822
BJC	54,795	3288	109589	2740	4110	3288	54,795	0	3288	219178	16,4384	548
BDC	3288	1096	5479	548	2466	1096	3288	5479	0	8219	4110	274
SJZC	16438	2740	219178	5479	6849	10,959	219178	273973	10,959	0	136986	8219
JNC	24,658	3288	273973	4110	6027	16,438	136986	219178	10,959	164384	0	5479
YTC	822	274	2740	274	274	548	822	1370	822	2740	548	0

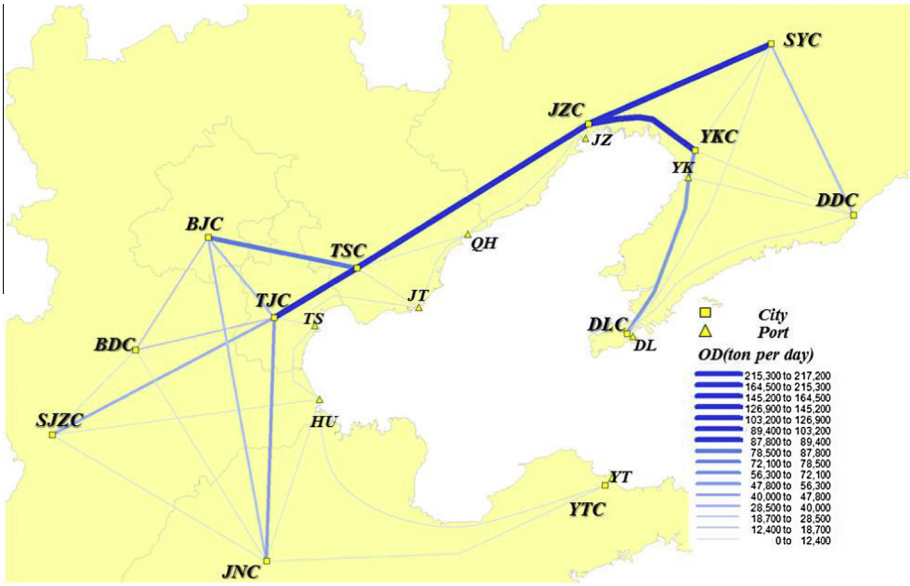

Fig. 16. Traffic flow pattern without routes.

the optimization calculations twenty times, acquiring twenty liner route schemes and their liner operation costs, amounts of required subsidy (BNS) and operator's profits. And then, among these schemes, we picked the scheme which needed the smallest amount of required subsidy, and used this scheme as the optimization result at the given minimum carbon-reduction rate. This process was repeated for each increase of the minimum carbon-reduction rate to acquire the final experiment results.

6.2. Analysis and discussion of results

We performed 16 tests for the different minimum carbon-reduction rates (EER: 15–30%). This led to 16 corresponding optimized route schemes. Table 2 lists the actual carbon-reduction rate (CER) achieved by the coastal shipping networks, operating cost (OC), profit excluding state subsidy (PWS), and required subsidy (BNS) of these schemes respectively. All monetary values are expressed in Chinese Yuan (CNY).

Fig. 17 shows the changes of the PWS, OC and BNS with the increase of the CER. The changing processes can be divided into two phases. In the first phase, when the CER rises from 15.21% to 27.14%, the PWS gradually decreases from 13,657 to −30,410 CNY per day; the OC slowly increases from 36,702 to 104,610 CNY per day; the BNS increases from 0 to 40,871 CNY per day. On average, every percent increase of the CER decreases the PWS by 3694 CNY per day, increases the OC by 5692 CNY per day and raises the BNS by 3426 CNY per day.

In the second phase corresponding to a CER rise between 27.70% and 30.82%, the PWS declines rapidly from −49,948 to −114,309 CNY per day, while the OC increases sharply from 123,630 to 190,200 CNY per day and the BNS jumps from 62,311 to 133,329 CNY per day. In this phase, each percent rise in the CER makes the PWS fall by 20,629 CNY per day on average, and

Table 2
Results under different carbon reduction target rates.

Test no.	EER (%)	CER (%)	OC (CNY/day)	PWS (CNY/day)	BNS (CNY/day)
1	15	15.21	36,702	13,657.69	0.00
2	16	16.12	38,040	13,295.48	0.00
3	17	17.23	42,041	11,029.57	0.00
4	18	18.67	57,060	2612.24	3093.76
5	19	19.56	47,550	−4258.24	9013.24
6	20	21.38	76,080	−12,148.51	19,756.51
7	21	21.80	66,570	−14,835.93	21,492.93
8	22	24.15	71,230	−19,544.67	26,667.67
9	23	24.21	73,880	−20,842.42	28,230.42
10	24	24.39	79,050	−21,030.94	28,935.94
11	25	27.14	104,610	−30,410.38	40,871.38
12	26	27.70	121,520	−50,159.29	62,311.29
13	27	27.75	114,120	−50,963.95	62,375.95
14	28	29.20	123,630	−59,977.31	72,340.31
15	29	29.75	152,160	−90,542.47	105,758.46
16	30	30.82	190,200	−114,309.53	133,329.53

leads the OC and the BNS to rise by 21,336 CNY per day and 22,762 CNY per day respectively. The decline rate of the PWS and the growth rate of the OC and the BNS are significantly higher compared to the first phase.

Next, we select three representative schemes (the schemes from Test 1, Test 11 and Test 16) to introduce how the coastal routing patterns change with the increment of the CER.

6.2.1. Liner service route pattern in Test 1 (EER = 15%)

Fig. 18 shows the coastal liner route and traffic flow pattern in Test 1. Three ships of 6000 DWT each are operating in a line-bundling type of service calling at several ports along the route in order to provide a shipping service with a service frequency of one call per day in the northern Bohai Bay area. The forward sub-route is TS–QH–JZ–YK, and the backward sub-route is YK–JT–TS. This routing schedule requires no state subsidy, but decreases the carbon emission by only 15.21%. The liner service configuration can bring the operator good earnings. This result suggests that when the targeted emission reduction rate is low and state subsidies are lacking, operators are likely to build high frequency line-bundling circular routes featuring small ships that call at a limited number of ports. The results also point to rather 'thin' flows in the maritime network compared to very dense cargo flows on the highway system, particularly on the axis between Shenyang (SYC)–Jinzhou (JZC)–Tangshan (TSC)–Tianjin (TJC)–Beijing (BJC) and the highway connecting Dalian (DLC) to Yingkou (YKC). The modal split in Test 1 thus strongly relies on road transportation.

6.2.2. Liner service route pattern in Test 11 (EER = 25%)

Fig. 19 displays the route structure and traffic flow pattern for Test 11. This time, 5 ships with a unit capacity of 20,000 dwt each are deployed in a pendulum-like service which connects all the major ports in the northern Bohai Bay. The forward sub-route is JT-QH-TS-HU-YT-JZ, and the backward sub-route is JZ-YT-HU-TS-QH-JT. Due to the availability of some state subsidies, the coastal shipping operator adopts a more complex liner-service structure using bigger ships. The combination

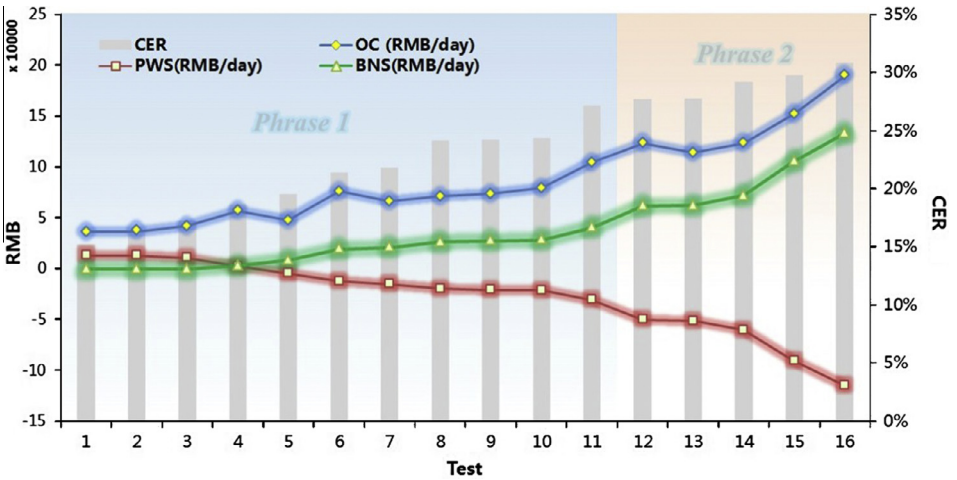

Fig. 17. Changes of the OC, PWS and BNS.

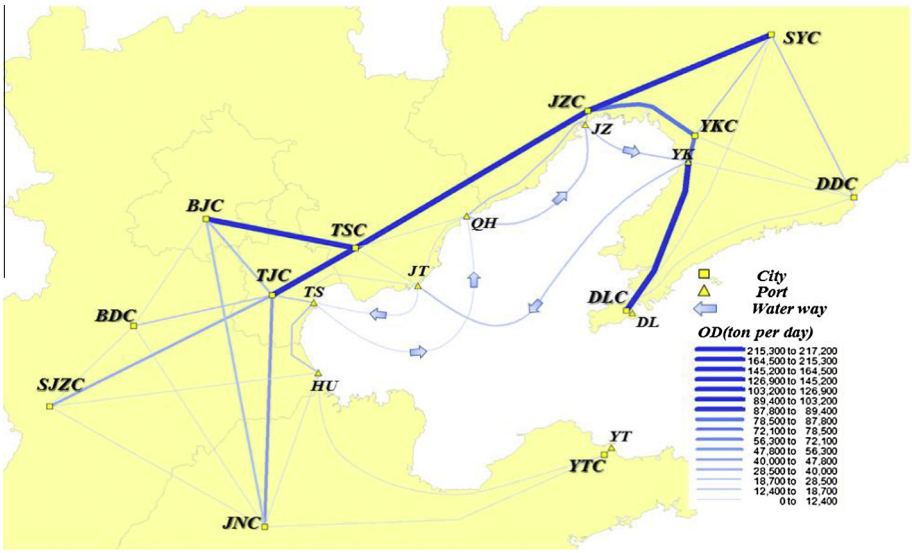

Fig. 18. Route scheme and traffic flow pattern in Test 1.

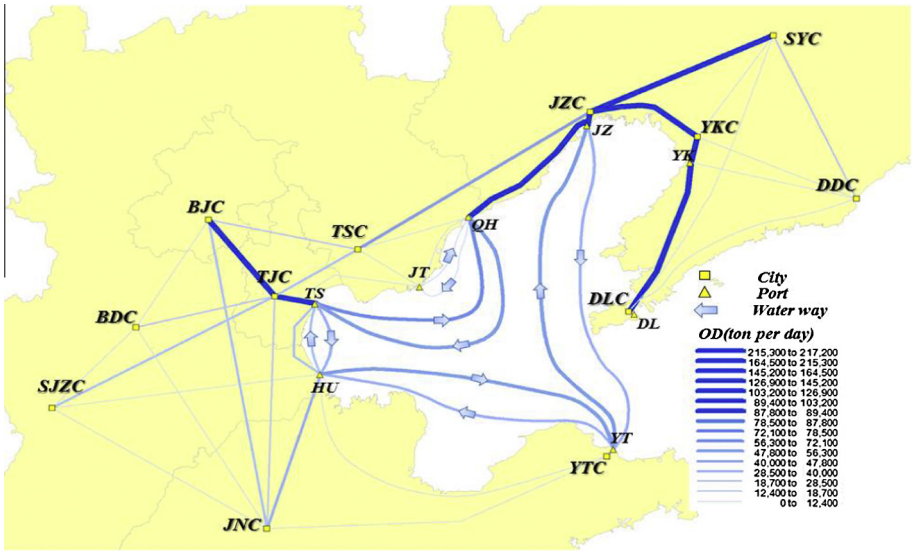

Fig. 19. Route scheme and traffic flow pattern in Test 11.

of larger ships and a more comprehensive maritime network increases the service level, port connectivity and the availability of the waterway transport system. As a result, significant traffic flows are now using the intermodal (waterway + highway) option instead of the 'truck only' option. Compared to Test 1 the maritime flows now reach a substantial level while long-distance highway traffic between inland cities is significantly lower, particularly on the Tangshan (TSC)–Tianjin (TJC) stretch of the highway system. The observed modal shift from road to sea increases the CER to 27.1%.

6.2.3. Liner service route pattern in Test 16

Fig. 20 shows the results for Test 16. A total of 17 ships of 20,000 DWT call at all major ports with a very high service frequency of four calls per day at each port. The forward sub-route is HU-TS-JT-YK-DL and the backward sub-route is DL-YT-QH-JZ-HU-TS. This liner route covers the whole region, and results in three high capacity and high frequency waterway corridors. Corridor 1 links Tianjin Port (TS) to Yingkou port (YK) via Jingtang port (JT). Corridor 2 goes from Jinzhou port (JZC) to Tianjin port (TS) via Huanghua (HU). Corridor 3 connects Yantai port (YT) to Qinhuangdao (QD). The depicted route scheme is very competitive attracting a lot of transport demand especially on the longer OD relations. The CER decreases significantly (as high as 30.82%). However, the operators face very high costs linked to the operation of this extensive shipping network requiring significant government subsidies to keep freight rates competitive.

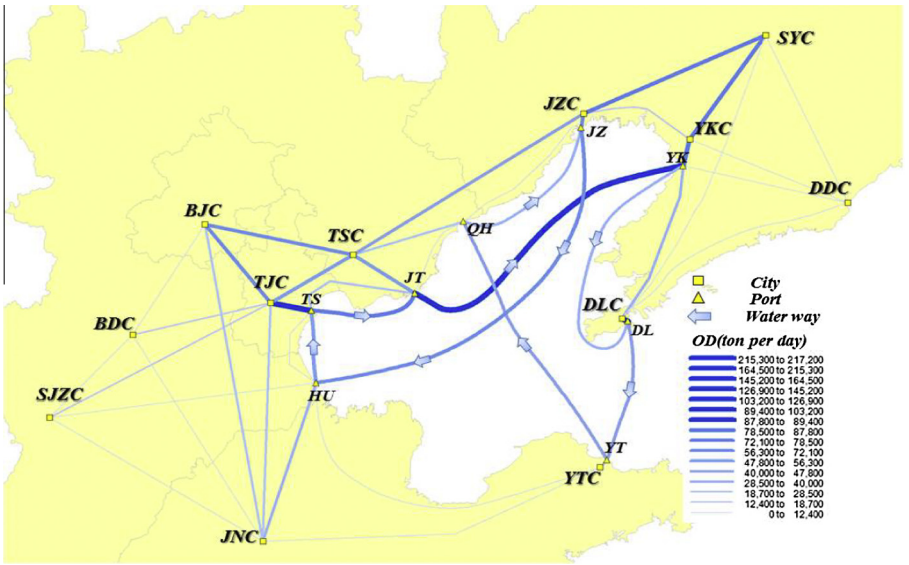

Fig. 20. Route scheme and traffic flow pattern in Test 16.

When comparing the above liner route schemes, it becomes clear that with the increment of the EER, the structure of the coastal shipping network becomes more and more complex. This is in line with our expectations.

7. Conclusions

Transport policy makers embrace coastal shipping as a means to mitigate landside congestion and to reduce greenhouse gas emissions per ton-mile. Governments have a range of legislative and regulatory tools at their disposal to support the competitiveness of coastal shipping. Carbon emission reduction targets and state subsidies for ship operators are part of this toolbox. Based on the user equilibrium assignment model (UE model), a New Coastal Liner Route Design Model (NCLRDM) was developed for intermodal networks characterized by competition between trucks and coastal shipping services. This paper addressed the CLRD problem from the perspective of controlling state subsidy levels against the backdrop of specific carbon emission reduction targets. Lower state subsidies might lead to higher profits for the ship operators if all other cost and revenue components remain unchanged. However, by explicitly considering the state subsidy issue in the analysis, instead of only focusing on maximizing profit levels or minimizing costs, the paper gains policy relevance. In this paper, we first proposed a traffic assignment method which fully considers the differences between waterway and highway links. Next, the NCLRDM was presented using mathematical expressions and the GFWHA was developed.

The main contributions of this paper are situated in two areas. Firstly, this paper introduces the NCLRDM. Through simulating the relationships between the government, ship operators and cargo owners, this model generates the optimal route scheme, a reasonable amount of state subsidy and transporting paths of each OD pairs at the point where the three stakeholders are in the state of equilibrium. The NCLRDM not only determines the ports of call, the call sequence, the ship type and the service frequency simultaneously, it does so with the objective of minimizing state subsidies under the requirement of specific carbon emission reduction targets. Secondly, based on the Temporal–Spatial Expansion, the paper introduces a new UE assignment method, which captures differences in traffic assignment between the maritime/waterway network and the highway network. The method represents a new avenue for assigning traffic on liner-type networks that involve high capacity transport units operating on fixed and scheduled paths.

The paper also provides case-based results relevant to policy makers. The model was empirically tested using a real-life case study on coastal liner service optimization in the Bohai Bay region in China. The empirical results show that higher emission reduction targets combined with state subsidies are likely to enhance the development of a more complex and comprehensive coastal shipping network. The resulting maritime corridors have the potential to significantly reduce trucking, particularly on long-distance highway corridors between inland cities.

The paper offers opportunities for further research. First, an application of the model to other regions and case studies around the world would shed more light on the external validity of the empirical results presented in this paper. In other words, a wider geographical focus will be beneficial to test the model specifications under different policy and market environments and to draw more generic conclusions on the interaction between coastal liner service design, carbon emission levels and the use of state subsidies. Secondly, the CLRD problem focused on a bimodal network configuration consisting of road transport and coastal shipping. Other transport modes such as rail transport and inland waterway or river transport were not considered. Future research efforts could be directed towards the extension of the intermodal network configura-

tion to include more transportation modes and their respective traffic assignment properties. Thirdly, when setting Eq. (5) of the NCLRDM, it is assumed that the relationship between the water transport price and the transport demand can be described with a BPR style function following a simple application of general economic law. However, the real relationship may be more complicated thereby opening avenues for further research.

References

Agarwal, R., Ergun, Ö., 2008. Ship scheduling and network design for cargo routing in liner shipping. Transportation Science 42 (2), 175–196.

Brooks, M.R., Trifts, V., 2008. Short sea shipping in North America: understanding the requirements of Atlantic Canadian shippers. Maritime Policy and Management 35 (2), 145–158.

Cho, S.-C., Perakis, A., 1996. Optimal liner fleet routing strategies. Maritime Policy and Management 23 (3), 249–259.

Christiansen, M., Fagerholt, K., Ronen, D., 2004. Ship routing and scheduling: status and perspectives. Transportation Science 38 (1), 1–18.

Claessens, E.M., 1987. Optimization procedures in maritime fleet management. Maritime Policy and Management 14 (1), 27–48.

Cominetti, R., Correa, J., 2001. Common-lines and passenger assignment in congested transit networks. Transportation Science 35 (3), 250–267.

Daly, A., 1999. The use of schedule-based assignments in public transport modelling. Proceedings of 27th European Transportation Forum, pp. 149–157.

De Cea, J., Fernández, E., 1993. Transit assignment for congested public transport systems: an equilibrium model. Transportation Science 27 (2), 133–147.

Dong, J.X., Song, D.P., 2009. Container fleet sizing and empty repositioning in liner shipping systems. Transportation Research Part E: Logistics and Transportation Review 45 (6), 860–877.

Douet, M., Cappuccilli, J.F., 2011. A review of short sea shipping policy in the European Union. Journal of Transport Geography 19 (4), 968–976.

European Union, 2008. Communication from the Commission providing guidance on State aid complementary to Community funding for the launching of the Motorways of the Sea. Official Journal of the European Union. 2008/C 317/08, pp. 10–12.

Fagerholt, K., 1999. Optimal fleet design in a ship routing problem. International Transactions in Operational Research 6 (5), 453–464.

Fagerholt, K., 2004. Designing optimal routes in a liner shipping problem. Maritime Policy and Management 31 (4), 259–268.

Florian, M., 1998. Deterministic time table transit assignment. Paper read at Preprints of PTRC Seminar on National Models.

García-Menéndez, L., Feo-Valero, M., 2009. European common transport policy and short-sea shipping: empirical evidence based on modal choice models. Transport Reviews 29 (2), 239–259.

Hamdouch, Y., Lawphongpanich, S., 2008. Schedule-based transit assignment model with travel strategies and capacity constraints. Transportation Research Part B: Methodological 42 (7), 663–684.

Hsu, C.-I., Hsieh, Y.-P., 2007. Routing, ship size, and sailing frequency decision-making for a maritime hub-and-spoke container network. Mathematical and Computer Modelling 45 (7), 899–916.

Jaramillo, D., Perakis, A.N., 1991. Fleet deployment optimization for liner shipping: Part 2. Implementation and results. Maritime Policy and Management 18 (4), 235–262.

Lam, W.H.-K., Gao, Z., Chan, K., Yang, H., 1999. A stochastic user equilibrium assignment model for congested transit networks. Transportation Research Part B: Methodological 33 (5), 351–368.

Lane, D., Heaver, T.D., Uyeno, D., 1987. Planning and scheduling for efficiency in liner shipping. Maritime Policy and Management 14 (2), 109–125.

Last, A., Keak, S., 1976. Transept: a bus model. Traffic Engineering and Control 17 (1).

Liu, X., Ye, H.-Q., Yuan, X.-M., 2011. Tactical planning models for managing container flow and ship deployment. Maritime Policy and Management 38 (5), 487–508.

López-Navarro, M.Á., Moliner-Tena, M.Á., Rodríguez-Artola, R.M., 2011. Long-term orientation of international road transport firms in their relationship with shipping companies: the case of short sea shipping. Transportation Journal 50 (4), 346–369.

Meng, Q., Wang, T., 2010. A chance constrained programming model for short-term liner ship fleet planning problems. Maritime Policy and Management 37 (4), 329–346.

Meng, Q., Wang, S., 2011a. Liner shipping service network design with empty container repositioning. Transportation Research Part E: Logistics and Transportation Review 44 (5).

Meng, Q., Wang, X., 2011b. Intermodal hub-and-spoke network design: incorporating multiple stakeholders and multi-type containers. Transportation Research Part B: Methodological 45 (4), 724–742.

Ng, A.K.Y., 2009. Competitiveness of short sea shipping and the role of port: the case of North Europe. Maritime Policy and Management 36 (4), 337–352.

Nielsen, O., Jovicic, G., 1999. A large scale stochastic timetable-based transit assignment model for route and sub-mode choices. In: Transportation Planning Methods. Proceedings of Seminar F, European Transport Conference, 27–29 September 1999, Cambridge, UK.

Notteboom, T., 2010. Concentration and the formation of multi-port gateway regions in the European container port system: an update. Journal of Transport Geography 18 (4), 567–583.

Notteboom, T., 2011. The impact of low sulphur fuel requirements in shipping on the competitiveness of roro shipping in Northern Europe. WMU Journal of Maritime Affairs 10 (1), 63–95.

Nuzzolo, A., Russo, F., 1996. Stochastic assignment models for transit low frequency services: some theoretical and operative aspects. In: Advanced Methods in Transportation Analysis. Springer, pp. 321–339.

Nuzzolo, A., Russo, F., Crisalli, U., 2001. A doubly dynamic schedule-based assignment model for transit networks. Transportation Science 35 (3), 268–285.

Nuzzolo, A., Crisalli, U., Rosati, L., 2012. A schedule-based assignment model with explicit capacity constraints for congested transit networks. Transportation Research Part C: Emerging Technologies 20 (1), 16–33.

Papola, N., Filippi, F., Gentile, G., Meschini, L., 2009. Schedule-based transit assignment: new dynamic equilibrium model with vehicle capacity constraints. Schedule-Based Modeling of Transportation Networks, 1–26.

Perakis, A.N., Denisis, A., 2008. A survey of short sea shipping and its prospects in the USA. Maritime Policy and Management 35 (6), 591–614.

Perakis, A., Jaramillo, D., 1991. Fleet deployment optimization for liner shipping: Part 1. Background, problem formulation and solution approaches. Maritime Policy and Management 18 (3), 183–200.

Poon, M., Wong, S., Tong, C., 2004. A dynamic schedule-based model for congested transit networks. Transportation Research Part B: Methodological 38 (4), 343–368.

Powell, B., Perkins, A., 1997. Fleet deployment optimization for liner shipping: an integer programming model. Maritime Policy and Management 24 (2), 183–192.

Rana, K., Vickson, R., 1988. A model and solution algorithm for optimal routing of a time-chartered containership. Transportation Science 22 (2), 83–95.

Rana, K., Vickson, R., 1991. Routing container ships using Lagrangean relaxation and decomposition. Transportation Science 25 (3), 201–214.

Ronen, D., 1983. Cargo ships routing and scheduling: survey of models and problems. European Journal of Operational Research 12 (2), 119–126.

Ronen, D., 1993. Ship scheduling: the last decade. European Journal of Operational Research 71 (3), 325–333.

Sambracos, E., Paravantis, J.A., Tarantilis, C.D., Kiranoudis, C.T., 2004. Dispatching of small containers via coastal freight liners: the case of the Aegean Sea. European Journal of Operational Research 152 (2), 365–381.

Schmöcker, J.-D., Bell, M.G., Kurauchi, F., 2008. A quasi-dynamic capacity constrained frequency-based transit assignment model. Transportation Research Part B: Methodological 42 (10), 925–945.

Sheffi, Y., 1984. Urban Transportation Networks: Equilibrium Analysis with Mathematical Programming Methods. Prentice Hall.

Shintani, K., Imai, A., Nishimura, E., Papadimitriou, S., 2007. The container shipping network design problem with empty container repositioning. Transportation Research Part E: Logistics and Transportation Review 43 (1), 39–59.
Spiess, H., Florian, M., 1989. Optimal strategies: a new assignment model for transit networks. Transportation Research Part B: Methodological 23 (2), 83–102.
Sumalee, A., Tan, Z., Lam, W.H., 2009. Dynamic stochastic transit assignment with explicit seat allocation model. Transportation Research Part B: Methodological 43 (8), 895–912.
Surry, P.D., Radcliffe, N.J., Boyd, I.D., 1995. A multi-objective approach to constrained optimization of gas supply networks: the COMOGA method. In: Evolutionary Computing. Springer, pp. 166–180.
Tong, C., Wong, S., 2000. A predictive dynamic traffic assignment model in congested capacity-constrained road networks. Transportation Research Part B: Methodological 34 (8), 625–644.
Wilson, N.H., Nuzzolo, A., 2009. Schedule-based Modeling of Transportation Networks: Theory and Applications. Springer.
Wong, S., Tong, C., 1998. Estimation of time-dependent origin–destination matrices for transit networks. Transportation Research Part B: Methodological 32 (1), 35–48.
Wu, J.H., Florian, M., Marcotte, P., 1994. Transit equilibrium assignment: a model and solution algorithms. Transportation Science 28 (3), 193–203.
Yamada, T., Russ, B.F., Castro, J., Taniguchi, E., 2009. Designing multimodal freight transport networks: a heuristic approach and applications. Transportation Science 43 (2), 129–143.
Yan, S., Chen, C.-Y., Lin, S.-C., 2009. Ship scheduling and container shipment planning for liners in short-term operations. Journal of Marine Science and Technology 14 (4), 417–435.
Yang, Z., Chen, K., Notteboom, T., 2012. Optimal design of container liner services: interactions with the transport demand in ports. Maritime Economics & Logistics 14 (4), 409–434.